Original Article
Dl-3-n-butylphthalide improves functional recovery in rats with spinal cord injury by inhibiting endoplasmic reticulum stress-induced apoptosis

Zili He[1,2*], Yulong Zhou[1,2*], Yan Huang[2*], Qingqing Wang[1], Binbin Zheng[1,6], Hongyu Zhang[2,3], Jiawei Li[1], Yanlong Liu[2], Fenzan Wu[4], Xie Zhang[5], Songlin Tong[4], Maofeng Wang[3], Zhouguang Wang[2], Huacheng He[2], Huazi Xu[1], Jian Xiao[1,2]

[1]Department of Orthopaedics, The Second Affiliated Hospital, Wenzhou Medical University, Wenzhou 325035, Zhejiang, PR China; [2]Molecular Pharmacology Research Center, School of Pharmacy, Wenzhou Medical University, Wenzhou 325035, Zhejiang, PR China; [3]Department of Biomedical Sciences Laboratory, Affiliated Dongyang Hospital of Wenzhou Medical University, Dongyang 322100, Zhejiang, PR China; [4]Department of Neurosurgery, Affiliated Cixi People's Hospital, Wenzhou Medical University, Ningbo 315300, PR China; [5]Department of Gastroenterology, Ningbo Medical Treatment Center Li Hui-Li Hospital, Ningbo 315040, PR China; [6]Department of Orthopaedics, Taizhou Hospital, Wenzhou Medical University, Linhai 317000, Zhejiang, PR China. *Equal contributors.

Abstract: Endoplasmic reticulum (ER) stress-induced apoptosis occurs in the spinal cord following traumatic spinal cord injury (SCI). Dl-3-n-butylphthalide (NBP) exerts an neuroprotective effects against both ischemic brain injury and neurodegenerative diseases; however, the relationship between ER stress-induced apoptosis and the therapeutic effect of NBP in SCI remains unclear. In this study, moderate spinal cord injuries were induced in Sprague-Dawley (SD) rats with a vascular clip. NBP was administered by oral (80 mg/kg/d) gavage 2 h before injury and then once daily for 28 d thereafter. Neurological recovery was assessed using the Basso, Beattie, and Bresnahan (BBB) locomotion rating scale, the inclined plane test, and the footprint analysis. Neuronal cell death was examined by TUNEL staining at 7 days post-injury. ER stress and apoptosis-related proteins were quantified by immunofluorescence staining and western blotting both *in vivo* and *in vitro*. Our results showed that NBP significantly decreased spinal cord lesion cavity area and improved locomotor recovery in SD rats after SCI. NBP also decreased neuronal apoptosis and inhibited activation of the caspase 3 cascade. Upregulation of ER stress-related proteins, such as GRP78, ATF-6, ATF-4, PDI, XBP-1, and CHOP, was reversed by NBP treatment in SD rats with SCI. Similarly, NBP effectively ameliorated ER stress and apoptosis-related protein expression induced by incubation with thapsigargin (TG) in PC12 cells. Our findings demonstrate that NBP treatment alleviates secondary SCI by inhibiting ER stress-induced apoptosis, thereby promoting neurological and locomoter functional recovery.

Keywords: Dl-3-n-butylphthalide, apoptosis, ER stress, spinal cord injury

Introduction

Spinal cord injury (SCI) is a severe health problem that usually results in lifelong disability. Many secondary detrimental injuries induced by SCI are characterized by loss of sensory, motor, and autonomic function, which are distal to the level of injury. Thus, SCI poses an immense economic and psychological burden worldwide. The pathology of SCI is divided into two phases: the primary injury, which involves disruption of spinal cord tissue, and the secondary injury, which involves a complex cascade of molecular events resulting in distur-

bances of ionic homeostasis leading local edema, focal hemorrhage, oxidative stress, inflammation, and extensive neuronal death [1]. A substantial amount of research over the past decade has been conducted to develop therapeutic intervention to treat the secondary damage from SCI [2]. Several animal studies have suggested that extensive cell death plays a pivotal role in mediating progressive spinal cord degeneration as the secondary spinal cord damage [3]. Although the exact mechanisms underlying secondary spinal cord damage remain unclear, inhibiting or delaying extensive neuronal death may represent an effective

therapeutic strategy to treat the secondary injury following SCI.

The endoplasmic reticulum (ER) is an important subcellular organelle that facilitates proper folding of newly synthesized secretory and membranous proteins and also regulates intracellular Ca^{2+} storage [4]. Many pathological changes associated with the secondary spinal cord injury are linked with unfolded or misfolded protein aggregation and protein glycosylation disruption secondary, which may cause ER stress and trigger the unfolded protein response (UPR). Previous studies have shown that the UPR is an adaptive mechanism plays an important role in cell growth, differentiation and apoptosis [5-7]. Several studies have shown that ER stress-induced cell death occurs in the spinal cord after a transient ischemia or a traumatic injury [1, 8, 9]. Although the etiology of SCI is complicated, it has been suggested that down-regulation of ER stress might be possible to reduce neuronal death and to improve patient outcomes following SCI.

L-3-n-butylphthalide is an extract from seeds of Chinese celery Apium graveolens Linn. DL-3-n-butylphthalide (NBP) can be chemically synthesized and is widely used to treat stroke patients. Multiple studies have demonstrated that NBP exerts a neuroprotective effect via multiple cellular processes, which were associated with reduced oxidative damage [10, 11], improved mitochondrial function [12], attenuated neuronal death [13-15] and anti-inflammation [16]. Furthermore, NBP alleviated b-amyloid-induced cell death in neuronal cell cultures [17], and improved cognitive performance in animal models of Alzheimer's disease [18]. Also, NPB prolonged animal survival rate by attenuating glial activation in a mouse model of amyotrophic lateral sclerosis [19]. However, much less is known regarding the neuroprotective effect of NBP in a model of acute SCI and its associated mechanisms.

In the present study, we investigated how NBP exerts its effect promoting neuroprotection, functional recovery, and neuronal survival after SCI. Our results indicated that NBP improves locomotor recovery by inhibiting ER stress-induced neural death in animals following SCI, which suggests that NBP is a possible therapeutic intervention to treat the secondary damage following SCI.

Materials and methods

Reagents and antibodies

NBP (purity > 99.5%) was provided by Shijiazhuang Pharmaceutical Group NBP Pharmaceutical Co., Ltd (Shijiazhuang, China). The TUNEL Apoptosis Assay Kit was purchased from Roche (Mannheim, Germany). NeuN, cleaved caspase 3, GRP78, ATF-6, ATF-4, PDI, XBP-1, and CHOP antibodies and goat anti-rabbit Alexa Fluor 488 antibody were purchased from Abcam. Goat anti-rabbit and anti-mouse IgG-HRP antibodies were purchased from Cell Signaling Technology, Inc. (Danvers, MA, USA). Dulbecco's modified Eagle medium (DMEM), FBS, penicillin and streptomycin were purchased from Invitrogen (Carlsbad, CA). All chemicals, including TG, were obtained from Sigma (Sigma-Aldrich, St.Louis, MO, USA).

Cell culture and viability assay

PC12 cells were purchased from the Cell Storage Center of Wuhan University (Wuhan, China). Cells were expanded and maintained in DMEM containing heat-inactivated 10% FBS, 5% horse serum, penicillin (final concentration, 100 U/ml), and streptomycin (final concentration, 0.1 mg/ml) in a humidified atmosphere of 5% CO_2 and 95% air at 37°C. NBP was dissolved in DMSO at a concentration of 8 mM. Cells were seeded on 96-well plates ($5×10^3$ cells/well) and treated with TG (10 µM) in the presence or absence of NBP or with NBP alone for 24 h. MTT (0.5 mg/ml) was added to the medium, which was incubated for an additional 4 h thereafter. At the end of the incubation period, the medium was removed, and 100 µl of DMSO was subsequently added to each well. The absorbance was measured at 570 nm. Cell viability was expressed as a percentage of the control culture (100%). All experiments were performed in triplicate.

Spinal cord injury model and NBP treatment

Female SD rats (220-250 g) were purchased from the Chinese Academy of Sciences, Shanghai, China (SCXK [Zhe] 2005-0019). All SD rats subjected to surgery were maintained in a temperature-controlled environment (23-25°C) with 12 h light/dark cycles and free access to food and water. SCI was introduced as previously described [20]. After animals

were anaesthetized with 2% (w/v) pentobarbital sodium (40 mg/kg), all fur and muscle adjacent to the spinous processes were dislodged to expose the vertebral column, and a laminectomy was performed at the T9 vertebral level to expose the spinal cord. Moderate contusions were created using a vascular clip (15 g forces, Oscar, China) for 1 min. Then, the incision site was closed in layers. In SCI+NBP rats, NBP diluted in peanut oil was administered by oral (80 mg/kg/d) gavage 2 h before injury and then once daily until animals were sacrificed. An equal dose of peanut oil was administered to vehicle-treated rats. Rats in the sham-operated group (n = 35) were subjected to the same surgical procedure, but without compression injury. Regarding postoperative care, manual urinary bladder emptying was performed twice daily until the bladder function was returned in animals. Animals were scarified on day 7 or day 28 following SCI.

Locomotion recovery assessment

After injury, functional deficit was scored using the 21-point Basso-Beattie-Bresnahan (BBB) locomotion scale, and was examined by performing the inclined plane test, and the footprint analysis. The BBB locomotion scale was conducted at 3, 7, 14 and 28 d after SCI. Animals were placed in an open experimental field and allowed to move freely for 5 min. Crawling ability was evaluated using the BBB scale ranging from 0 (no limb movement or weight support) to 21 (normal locomotion). The inclined plane test was performed at each indicated time point after SCI. Briefly, animals were tested in two positions (right-side or left-side up) on a testing apparatus (i.e., a board covered with a rubber mat containing horizontal ridges spaced 3 mm apart). At each position, the maximum angle at which a rat could retain its position for 5 s without falling was recorded, and these values were averaged to obtain a single score for each animal. For the footprint analysis, the hind paws for each animal were dipped in ink. Each animal was then allowed to walk across a narrow box (3 m long and 10 cm wide), and its footprints were scanned, and digitized images were analyzed.

Hematoxylin-eosin (HE) staining and Nissl staining

Rats (n = 5 per group) were anesthetized and transcardially perfused with 0.9% NaCl, followed by 4% paraformaldehyde (PFA) (dissolved in 0.01 M phosphate buffered saline, PBS, pH = 7.4) at 7 d after injury. The T7-T9 spinal cord segments near the lesion epicenter were collected and fixed in 4% (w/v) PFA for 24 h and embedded in paraffin for transverse sectioning. Then, 5 µm-thick sections were cut on poly-L-lysine-coated slides for histopathological examination. Sections were stained with hematoxylin and eosin for HE staining and cresyl violet for Nissl staining, in accordance with the manufacturer's instructions. Images are captured using a Nikon ECLPSE 80i (Nikon, Japan). HE staining was performed to quantify the epicenter cavity area, which was traced using contour mapping with IPP software. Nissl-positive cells were automatically counted in 5 randomly selected fields per sample in the ventral horn of the spinal cord and were quantified using IPP software.

Immunofluorescence staining

Sections were deparaffinized, rehydrated and washed twice for 15 min in PBS. For *in vitro* protein analysis, PC12 cells were grown on covers lips in 6-well plates. After treatment, cells were fixed in 4% (w/v) PFA for 15 min and then washed with PBS three times for 2 min each. Then, sections were incubated in 3% H_2O_2 for 15 min at room temperature and blocked with 5% bovine serum albumin in PBS containing 0.1% Triton X-100 at 37°C for 30 min. Sections were subsequently incubated with primary antibodies at 4°C overnight with appropriate dilutions (NeuN (neuronal marker) (1:800), cleaved caspase 3 (1:800), GRP78 (1:800), and PDI (1:800)). Then, sections were washed in PBS and incubated with goat anti-rabbit Alexa Fluor 488 secondary antibody at room temperature for 1 h. Nuclei were stained with DAPI for 7 min. Images were captured using a Nikon ECLPSE 80i (Nikon, Japan) at 400× magnification. A negative (no antibody) control was included [21].

Apoptosis assay

DNA fragmentation was detected *in vivo* using a one-step TUNEL Apoptosis Assay Kit. After deparaffinization and rehydration, sections were pretreated with 20 mg/ml proteinase-K in 10 mM Tris-HCl at 37°C for 15 min and then were incubated in 0.1% sodium citrate and 0.1% Triton X-100 solution for 10 min. After being washed with PBS, sections were incubat-
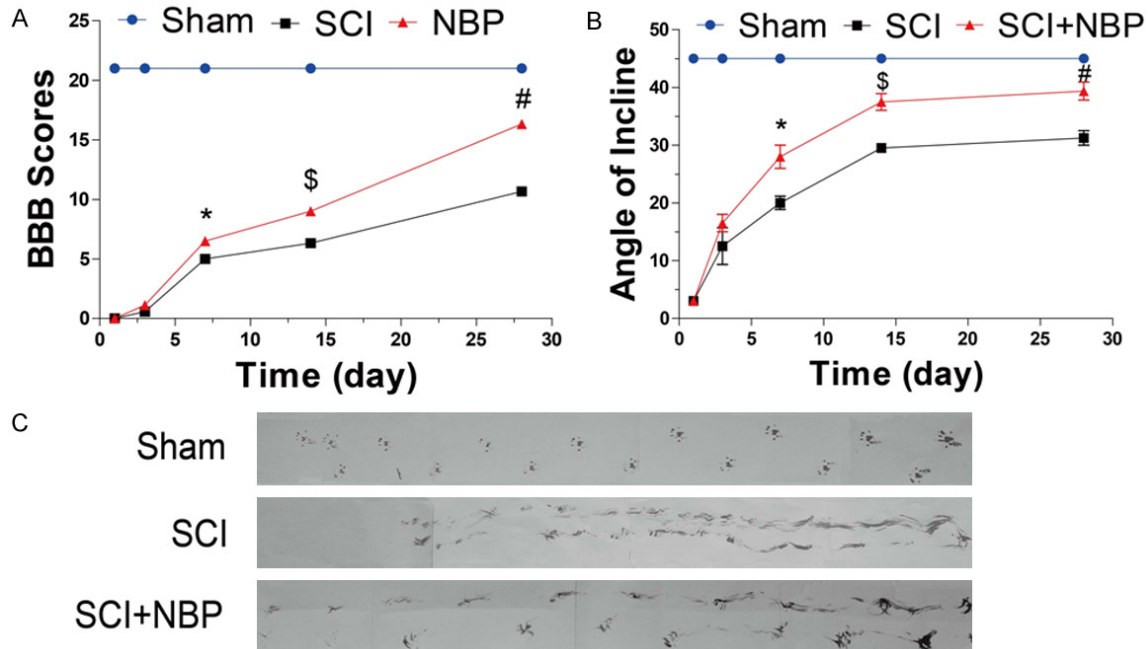
Figure 1. NBP facilitates improved recovery from spinal cord injury (SCI). After SCI, NBP was administered by oral (80 mg/kg/d) gavage once per day for 28 d, and recovery was assessed via the BBB locomotion scale, the inclined plane test, and footprint analysis. A. The BBB scores of the sham, SCI, and SCI+NBP groups (n = 8 per group). The score of the sham group was 21 points, which represents normal motor function. Data represent Mean values ± SEM, *P < 0.001 versus the SCI group, $P < 0.001 versus the SCI group, and #P < 0.001 versus the SCI group. B. The inclined plane test scores of the different groups (n = 8 per group). Data represent Mean values ± SEM, *P < 0.001 versus the SCI group, $P < 0.001 versus the SCI group, and #P < 0.001 versus the SCI group. C. Footprint analysis results of the different groups.

ed with 20 μl of TUNEL reaction mixture with terminal deoxynucleotidyltransferase (TdT) for 1 h at 37°C. Nuclei were stained with DAPI [22]. Images were visualized using a Nikon ECLPSE 80i (Nikon, Japan) at 400× magnification, and TUNEL-positive cells were automatically counted in 5 randomly selected fields in the ventral horn of the spinal cord in each sample and were quantified using IPP software.

Western blot analysis

Protein from animals or PC12 cells were purified using protein extraction reagents. An equivalent of 70 μg of protein was separated by 11.5% (w/v) gel and transferred onto a PVDF membrane (Bio-Rad Laboratories). Membranes were blocked with 5% freshly prepared milk-TBST for 90 min at room temperature and then were incubated overnight at 4°C with primary antibodies (cleaved caspase 3 (1:1000), GRP78 (1:1000), ATF-6 (1:1000), ATF-4 (1:1000), PDI (1:1000), XBP-1 (1:1000), and CHOP (1:1000)). After being washed in TBST, membranes were incubated with the goat anti-rabbit secondary antibody for 1 h at room temperature, and

bands were detected using an enhanced chemiluminescence (ECL) kit [23, 24]. Band intensity was quantified using Image Lab 3.0 software (Bio-Rad). Experiments were repeated three times [25].

Statistical analysis

Data are presented as the mean ± SEM. Statistical significance was determined by Student's t-test if comparing only two groups or one way ANOVA followed by Bonferroni's multiple comparisons test if analyzing more than two groups. The BBB locomotor scores and the inclined plane test scores were analyzed using Two-way ANOVA followed by Bonferroni post-hoc comparison test. Differences were considered to be statistically significant when P < 0.05.

Results

NBP improves locomotor functional recovery after SCI in rats

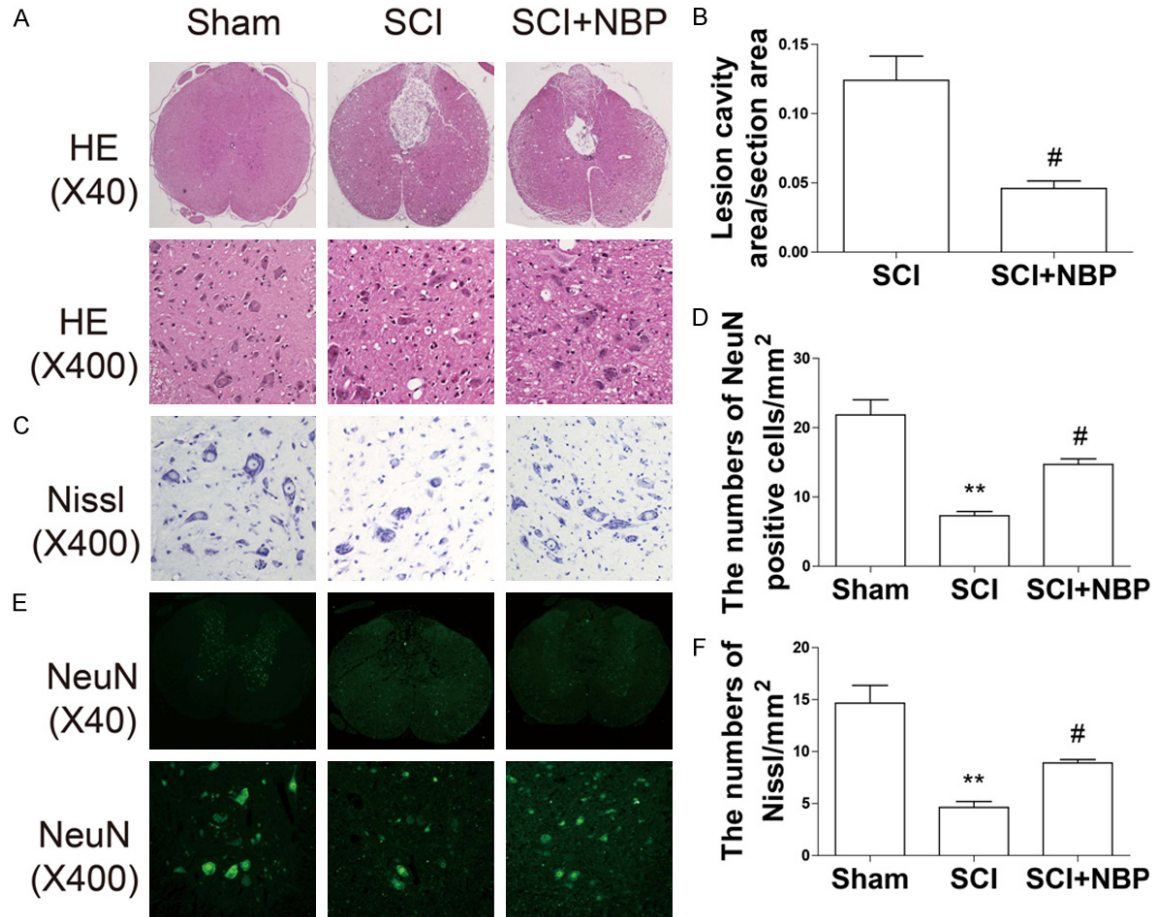To evaluate the therapeutic effect of NBP on SCI, rats were treated with NBP by oral gavage.

Figure 2. NBP reduces lesion volume and motor neuron loss after SCI. At 7 d after SCI, sections of injured spinal cord were assessed via HE staining, Nissl staining, and immunofluorescence staining for NeuN. A. HE staining results for the sections of injured spinal cord in the sham, SCI, and SCI+NBP groups. B. Quantification analysis of lesion cavity area in the SCI and NBP groups. Data represent Mean values ± SEM, #P < 0.05 versus the SCI group, n = 5 per group. C. Nissl staining results in the ventral horn of the spinal cord in the different groups at 7 d after SCI. D. Quantification analysis of the number of Nissl-stained cells. Data represent Mean values ± SEM, **P < 0.01 versus the sham group, and #P < 0.05 versus the SCI group, n = 5 per group. E. Immunofluorescence staining for NeuN in the different groups. F. Quantification analysis of the number of NeuN-positive cells. Data represent Mean values ± SEM, **P < 0.01 versus the sham group, and #P < 0.05 versus the SCI group, n = 5 per group.

The BBB locomotion scale, the inclined plane test, and the footprint analysis were used to evaluate locomotor recovery in SD rats following SCI. Sham-operated controls represented normal motor function, which was signified by a score of 21. Based on the BBB locomotion scale results, there was no significant difference between the SCI+NBP and SCI groups at 1 and 3 d after injury. However, with an extended observation, we noted that NBP-treated rats scored better than those of vehicle-treated rats (n = 8 per group; BBB rating scale: 7 days, NBP vs SCI, 6.500 ± 0.1890 vs 4.875 ± 0.2266, *P < 0.001; 14 days, NBP vs SCI, 8.875 ± 0.2266 vs 6.375 ± 0.1830, $P < 0.001; 28 days, NBP

vs SCI, 16.38 ± 0.2631 vs 10.75 ± 0.2500, #P < 0.001) (Figure 1A) at 7, 14 and 28 d after injury. Consistent with these findings, the inclined plane test also showed that the maximum angles were markedly higher in the SCI+NBP group than in the SCI group at 7, 14 and 28 d after injury (n = 8 per group; maximum angles: 7 days, NBP vs SCI, 28.00 ± 1.309 vs 20.00 ± 0.7559, *P < 0.001; 14 days, NBP vs SCI, 37.50 ± 0.9449 vs 29.50 ± 0.3273, $P < 0.001; 28 days, NBP vs SCI, 39.38 ± 1.030 vs 31.25 ± 0.8183, #P < 0.001) (Figure 2B). NBP-treated rats showed fairly consistent hindlimb coordination and a few toe dragging at 28 d after SCI. In contrast, vehicle-treated animals
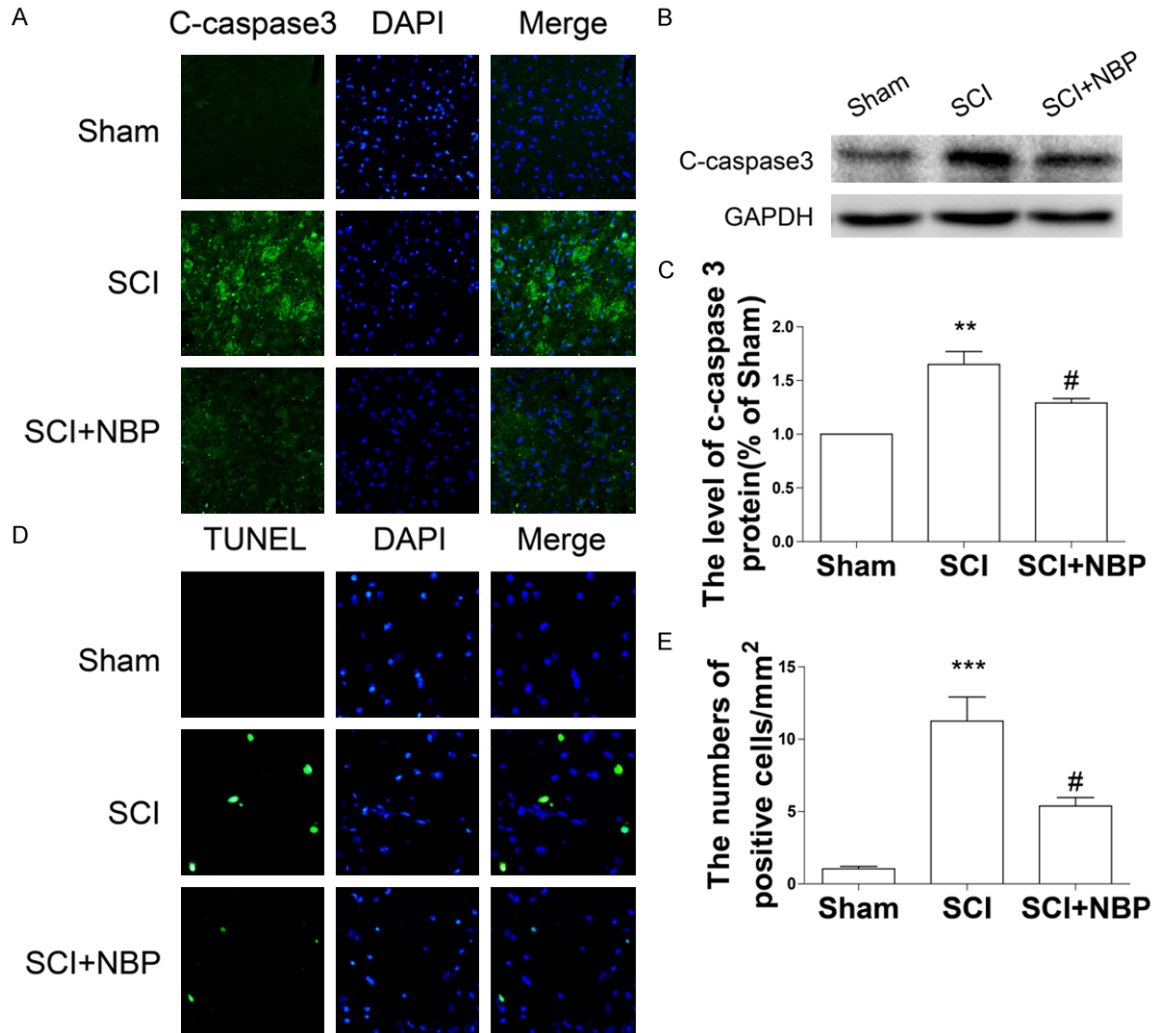
Figure 3. NBP attenuates apoptosis after SCI. A. Immunofluorescence staining of cleaved caspase 3 in sections from the ventral horn of the spinal cord in the sham, SCI, and SCI+NBP groups at 7 d after SCI (magnification ×400). B, C. Protein expression and quantification analysis of cleaved caspase 3 in segments of injured spinal cord in the different groups at 7 d after SCI. Data represent Mean values ± SEM, **P < 0.01 versus the sham group, and #P < 0.05 versus the SCI group, n = 5 per group. D. TUNEL staining results in sections from the ventral horn of the spinal cord in the different groups at 7 d after SCI (magnification ×800). E. Quantification analysis of the number of TUNEL-positive cells. Data represent Mean values ± SEM, ***P < 0.001 versus the sham group, and #P < 0.01 versus the SCI group, n = 5 per group.

showed inconsistent coordination and extensive dragging, as demonstrated by the presence of ink streaks extending from both hindlimbs (**Figure 1C**).

NBP reduces lesion volume and loss of motor neurons after SCI in rats

To confirm the protective effect of NBP, we investigated neuronal survival directly via HE, Nissl, and immunofluorescence staining. HE staining showed that progressive dorsal white matter and central gray matter tissue destruc-

tion were observed in SCI rats at 7 d after injury. When compared with the SCI group, NBP-treated rats exhibited significantly less neuronal necrosis and karyopyknosis and smaller lesion cavity areas, indicating NBP has a neuroprotective effect (0.05096 ± 0.004722 vs 0.1186 ± 0.01456 #P < 0.01) (**Figure 2A**, **2B**). The effect of NBP on the number of motor neurons in the ventral horn of spinal cord was also investigated by Nissl staining and immunofluorescence staining. As shown in **Figure 2C-F**, the SCI group exhibited extensive loss of large Nissl-stained cells (**P < 0.01, **Figure 2C**, **2D**)
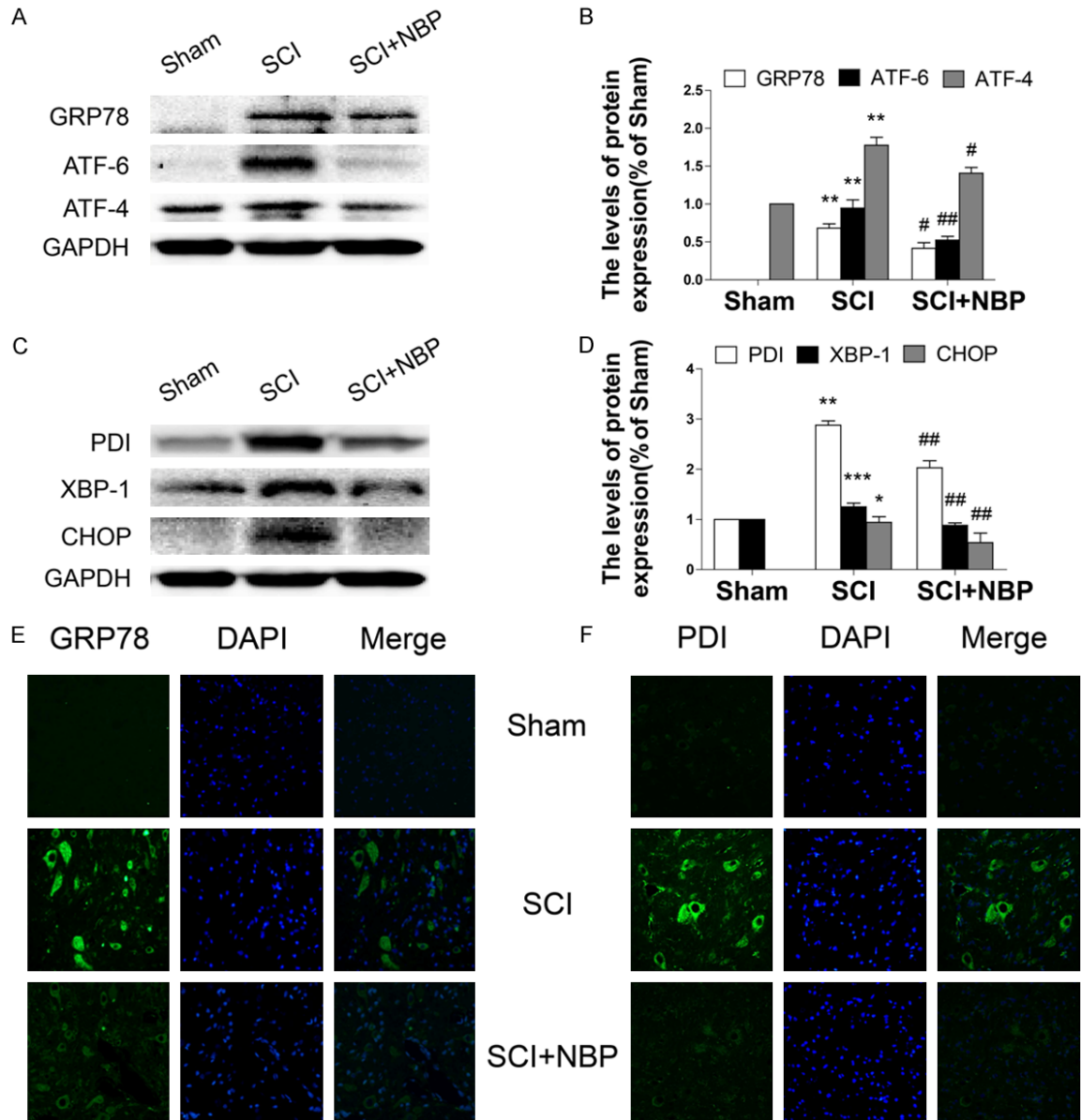
Figure 4. NBP inhibits activation of ER stress after SCI. A-D. Protein expression and quantification analysis of GRP78, ATF-6, ATF-4, PDI, XBP-1, and CHOP in segments of injured spinal cord in the sham, SCI, and SCI+NBP groups at 7 d after SCI. Data represent Mean values ± SEM, *P < 0.05, **P < 0.01, ***P < 0.001 versus the sham group, and #P < 0.05, ##P < 0.01 versus the SCI group, n = 5 per group. E, F. Immunofluorescence staining for cleaved caspase-3 in sections from the ventral horn of the spinal cord in the different groups at 7 d after SCI (magnification ×400).

and NeuN-positive cells (**P < 0.01, **Figure 2E, 2F**). In contrast, the number of Nissl-stained cells (#P < 0.05, **Figure 2C, 2D**) and NeuN-positive cells (#P < 0.05, **Figure 2E, 2F**) was sustained in the ventral horn of the spinal cord in the NBP-treated group after injury.

NBP attenuates neuronal apoptosis after SCI in rats

To determine whether the neuroprotective effect of NBP is related to apoptotic regulation,

apoptosis-related protein expression was measured by western blotting and immunofluorescence. As shown in **Figure 3A**, the optical density of cleaved caspase 3 in the ventral horn of the spinal cord at 7 d after SCI was dramatically increased in the SCI group when compared with the sham-operated group. However, this trend was reversed by NBP treatment. Similarly, cleaved caspase 3 protein expression was significantly decreased in the SCI+NBP group (#P < 0.01, **Figure 4B, 4C**). In both the SCI and the
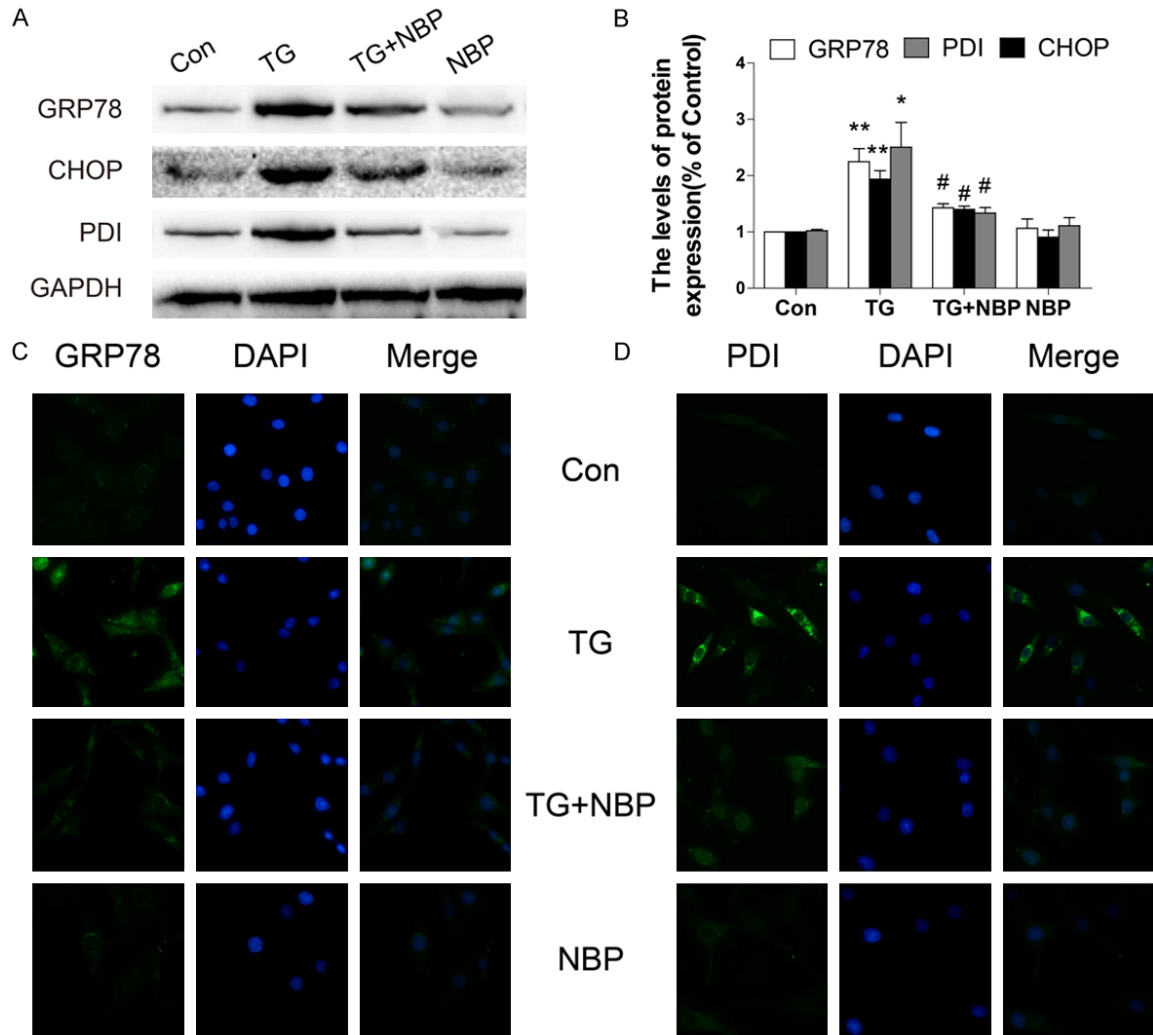
Figure 5. NBP inhibits TG-induced ER stress in PC12 cells. A, B. Protein expression and quantification analysis of GRP78, CHOP, and PDI in PC12 cells subjected to ER stress and treated with NBP. Data represent Mean values ± SEM, *P < 0.05, **P < 0.01 versus the control group, and #P < 0.05 versus the TG group, n = 3 per group. C, D. Immunofluorescence staining for GRP78 and PDI in PC12 cells subjected to ER stress and treated with NBP (magnification ×400).

SCI+NBP groups, TUNEL assay revealed extensive cell death at 7 d after injury. The number of TUNEL-positive cells in the ventral horn of the spinal cord at 7 d after injury was dramatically increased in the SCI group (***P < 0.001, **Figure 3D**, **3E**). However, significantly fewer TUNEL-positive cells were observed in NBP-treated rats as relative to vehicle-treated rats after injury (#P < 0.05, **Figure 3D**, **3E**). These results demonstrated that NBP administration suppressed neuronal apoptosis induced by SCI in rats.

NBP inhibits activation of ER stress after SCI in rats

A previous study demonstrated that prolonged ER stress could trigger cell death, which

occurred during the early stages of SCI [26]. We determined whether the anti-apoptotic effect of NBP is also associated with inhibition of ER stress-related protein expression in a animal model of SCI. We found that the levels of GRP7, ATF-6, ATF-4, PDI, XBP-1 and CHOP protein were significantly increased in rats following SCI as compared with those in the sham group (*P < 0.05, **P < 0.01, ***P < 0.001, **Figure 4A-D**). Interestingly, NBP-treated rats exhibited markedly decreased ER stress-related protein expression (#P < 0.05, ##P < 0.01, **Figure 4A-D**). We measured the immunofluorescence of GRP78 and PDI in the ventral horn of the spinal cordat 7 d in animals after SCI. Our results showed that the optical densities of GRP78 and PDI were significantly increased in the SCI
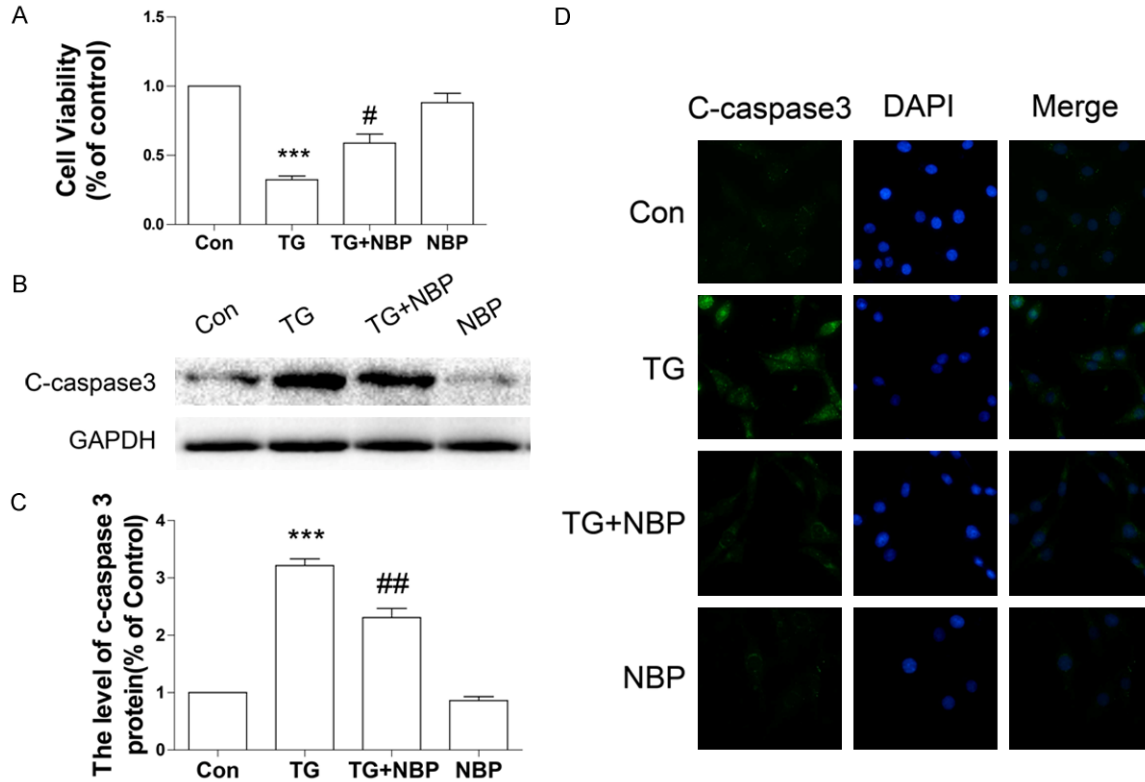
Figure 6. NBP attenuated TG-induced apoptosis in PC12 cells. A. MTT assay results for NBP-treated PC12 cells subjected to TG stimulation. Data represent Mean values ± SEM, ***P < 0.001 versus the control group, and #P < 0.05 versus the TG group, n = 3 per group. B, C. Protein expression and quantification analysis of cleaved caspase 3 in NBP-treated PC12 cells subjected to TG stimulation. Data represent Mean values ± SEM, ***P < 0.001 versus the control group, and ##P < 0.01 versus the TG group, n = 3 per group. D. Immunofluorescence staining for cleaved caspase-3 in NBP-treated PC12 cells subjected to TG treatment (magnification ×400).

group, which was significantly reversed by NBP treatment (**Figure 4E**, **4F**).

NBP inhibits TG-induced ER stress in PC12 cells

To confirm the inhibitory effect of NBP *in vitro,* PC12 *cells were treated with TG alone, or combined TG and NBP. Western blotting analyses showed that the le*vels of GRP78, CHOP, and PDI protein in PC12 cells were significantly increased at 24 h after TG stimulation (*P < 0.05, **P < 0.01, **Figure 5A**, **5B**), and the increase of ER stress-related protein expression induced by TG was markedly reversed by NBP treatment (#P < 0.05, **Figure 5A**, **5B**). Similarly, the optical densities of GRP78 and PDI as showed by immunostaining were markedly higher in TG-treated cells when compared to the control group. However, when cells were treated with NBP after TG stimulation, the opti-

cal densities of GRP78- and PDI were decreased (**Figure 5C**, **5D**).

NBP attenuates TG-induced cell death in PC12 cells

To confirm our hypothesis that the anti-apoptotic effect of NBP is related to inhibition of excessive ER stress *in vitro,* we performed an MTT assay and measured the level of cleaved caspase 3 protein in PC12 cells when treated with TG. A decrease in cell viability was observed in the group treated with TG alone (***P < 0.001, **Figure 6A**). However, treatment of NBP significantly promoted cell viability as compared with the TG-treated group (n = 3 per group; cell viability: NBP vs SCI, 58.79 ± 6.540% vs 32.33 ± 2.694% #P < 0.05, **Figure 6A**). Western blot analyses showed that the level of cleaved caspase 3 protein in PC12 cells was significantly increased at 24 h after TG treatment (***P <

0.001, **Figure 6B**, **6C**) and that treatment of NBP markedly decreased cleaved caspase 3 protein expression (##P < 0.01, **Figure 6B**, **6C**). These findings were further supported by the immunostainings (**Figure 6D**).

Discussion

NBP was approved by the State Food and Drug Administration of China for clinical use for treating ischemic stroke patients in 2002. Several lines of evidence have proven that in cerebral ischemia models, NBP facilitates microcirculation reconstruction [27, 28], infarct lesionsize reduction [29], and neurological injury attenuation [30], although mechanisms underlying these effects remain unclear. Recent studies have demonstrated that NBP significantly reduces oxidative damage [10, 11], improves mitochondrial function [12], reduces neuronal apoptosis [13-15] and inhibits inflammation [16]. In addition, the neuroprotective effect of NBP has been examined in animal models of many diseases, such as Alzheimer's disease [18], vascular dementia [31], diabetic cataracts [32], and amyotrophic lateral sclerosis (ALS) [19]. However, no studies so far have studied the neuroprotective effect of NBP in a model of acute SCI. In this study, we demonstrated that NBP effectively improved motor performance, improved neuronal survival, attenuated loss of motor neurons, and reduced infarct lesion sizes in rats following SCI.

SCI is characterized by various self-destructive processes resulting from disturbances in ionic homeostasis, which leads to local edema, focal hemorrhage, excitotoxicity, and the presence of free radicals and free fatty acids [1]. Extensive neuronal cell death (apoptosis) has been characterized as the secondary injury following SCI. Previous studies have showed that apoptosis occurs in neurocytes [33], endothelial cells [34], and all major glial sub-types (astrocytes, oligodendrocytes, and microglia) [6, 35, 36] after SCI, suggestingcell apoptosis may contribute greatly to the development of paralysis in patients following SCI. Thus, inhibition of cell apoptosis may be an effective therapeutic intervention for treating these patients. In the present study, the optical density of cleaved caspase 3 and the number of TUNEL-positive cells were dramatically increased in the ventral horn of the spinal cord at 7 d after

SCI when compared with the sham group. Treatment of NBP significantly reduced the levels of cleaved caspase 3 and TUNEL-positive cells in NBP-treated rats as compared with those in the non-treated SCI group. In a rat model of transient focal cerebral ischemia, treatment of NBP (20 mg/kg) reduced cytochrome c release, decreased Caspase-3 activity, and down-regulated DNA fragmentation [13]. Furthermore, administration of higher dose of NBP (60 mg/kg) facilitated motor neuron preservation when compared the treatment at a lower dose (30 mg/kg) in a mouse model of amyotrophic lateral sclerosis (ALS) [19]. Therefore, we speculate that oral administration of NBP elicits a neuroprotective effect in rats following SCI in a concentration-dependent manner.

Many pathological conditions, such as cellular injury or tissue ischemia, can cause ER stress [5]. During the early phase of ER stress, a self-protective signal transcription pathway is triggered which is characterized by an up-regulation of ER-localized molecular chaperone expression. In contrast, prolong ER stress precipitated by excessive noxious stimuli may trigger extensive cell death.

CHOP activates a pathway that induces cell apoptosis [7]. To confirm the signaling mechanism by which NBP inhibits neuronal apoptosis, we measured the levels of several ER stress-related proteins and found that the levels of GRP78, ATF-6, ATF-4, PDI, XBP-1 and CHOP were increased significantly following injury. Strikingly, these effects were reversed by treatment of NBP at 7 d after injury in rats. Consistent findings were observed in the in vitro study, treatment of NBP reversed TG-induced an increase of cleaved caspase 3, which lead to improved PC12 cell viability. These findings suggest that ER stress plays an important role in neuronal apoptosis induction after SCI and that NBP inhibits neuronal death by down-regulating ER stress. In our previous studies, we showed that bFGF and NGF improved functional recovery in rats with SCI by inhibiting ER stress-induced neuronal apoptosis [26, 37]. Our present findings suggest that NBP also inhibits neuronal apoptosis by regulating ER stress and that it has great potential for treating SCI [13, 15]. Unlike many preclinical drugs, the safety and stability of NBP have been

repeatedly demonstrated in clinical practice, repurposing our findings may significantly reduce the cost and time associated with new drug development for SCI patients.

Targeting the ER stress-related apoptotic signaling pathway may facilitate the development of new treatments for SCI in the future. However, in the present study we did not definitively elucidate the role of NBP in the inhibition of ER-stress induced neuronal apoptosis after SCI. In subsequent studies, we will focus on the signaling mechanism by which NBP inhibits ER stress-induced neuronal apoptosis. Furthermore, whether NBP inhibits neuronal apoptosis via the mitochondrial intrinsic pathway will be an additional focus of these studies. Many studies have shown that NBP reduces astrocytosis and microglial activation in animal models of ALS [19] and prevents disruption of the blood-brain barrier in rats after focal cerebral infarction [38]. Therefore, treatment of NBP might also decrease gliosis, inhibit inflammation, and maintain blood-spinal cord barrier integrity in rats following SCI.

In conclusion, we have demonstrated that NBP improved motor neuron survival by inhibiting cell apoptosis and thus accelerated locomotor functional recovery at 7 days in rats after SCI. We also found that the neuroprotective effect of NBP was related to the inhibition of ER stress induced by SCI. In addition, NBP significantly inhibited the ER stress-associated apoptotic pathway in TG-stimulated cells. These findings suggest that a therapeutic strategy targeting ER stress-related neuronal apoptosis may preserve locomotor function in rats following SCI and that NBP may be a novel therapeutic agent for treating SCI. The findings obtained in this study provide a basis for the future translation of NBP into clinical practice for treating SCI.

Acknowledgements

Disclosure of conflict of interest

None.

Address correspondence to: Jian Xiao, School of Pharmacy, Wenzhou Medical University, Wenzhou 325035, Zhejiang, PR China. Tel: +86-577-8577-3087; Fax: +86-577-85773087; E-mail: xfxj2000@126.com; Huazi Xu, Department of Orthopaedics, The Second Affiliated Hospital, Wenzhou Medical University, Wenzhou 325000, PR China. Tel: +86-577-88816381; Fax: +86-577-88816381; E-mail: spinexu@163.com

References

[1] Penas C, Guzman MS, Verdu E, Fores J, Navarro X and Casas C. Spinal cord injury induces endoplasmic reticulum stress with different cell-type dependent response. J Neurochem 2007; 102: 1242-1255.

[2] Thuret S, Moon LD and Gage FH. Therapeutic interventions after spinal cord injury. Nat Rev Neurosci 2006; 7: 628-643.

[3] Katoh K, Ikata T, Katoh S, Hamada Y, Nakauchi K, Sano T and Niwa M. Induction and its spread of apoptosis in rat spinal cord after mechanical trauma. Neurosci Lett 1996; 216: 9-12.

[4] Kim I, Xu W and Reed JC. Cell death and endoplasmic reticulum stress: disease relevance and therapeutic opportunities. Nat Rev Drug Discov 2008; 7: 1013-1030.

[5] Hoyer-Hansen M and Jaattela M. Connecting endoplasmic reticulum stress to autophagy by unfolded protein response and calcium. Cell Death Differ 2007; 14: 1576-1582.

[6] Valenzuela V, Collyer E, Armentano D, Parsons GB, Court FA and Hetz C. Activation of the unfolded protein response enhances motor recovery after spinal cord injury. Cell Death Dis 2012; 3: e272.

[7] Ohri SS, Maddie MA, Zhao Y, Qiu MS, Hetman M and Whittemore SR. Attenuating the endoplasmic reticulum stress response improves functional recovery after spinal cord injury. Glia 2011; 59: 1489-1502.

[8] Yamauchi T, Sakurai M, Abe K, Matsumiya G and Sawa Y. Impact of the endoplasmic reticulum stress response in spinal cord after transient ischemia. Brain Res 2007; 1169: 24-33.

[9] Sakurai M, Takahashi G, Abe K, Horinouchi T, Itoyama Y and Tabayashi K. Endoplasmic reticulum stress induced in motor neurons by transient spinal cord ischemia in rabbits. J Thorac Cardiovasc Surg 2005; 130: 640-645.

[10] Dong GX and Feng YP. Effects of NBP on ATPase and anti-oxidant enzymes activities and lipid peroxidation in transient focal cere-

bral ischemic rats. Zhongguo Yi Xue Ke Xue Yuan Xue Bao 2002; 24: 93-97.

[11] Li L, Zhang B, Tao Y, Wang Y, Wei H, Zhao J, Huang R and Pei Z. DL-3-n-butylphthalide protects endothelial cells against oxidative/nitrosative stress, mitochondrial damage and subsequent cell death after oxygen glucose deprivation in vitro. Brain Res 2009; 1290: 91-101.

[12] Huang JZ, Chen YZ, Su M, Zheng HF, Yang YP, Chen J and Liu CF. dl-3-n-Butylphthalide prevents oxidative damage and reduces mitochondrial dysfunction in an MPP(+)-induced cellular model of Parkinson's disease. Neurosci Lett 2010; 475: 89-94.

[13] Chang Q and Wang XL. Effects of chiral 3-n-butylphthalide on apoptosis induced by transient focal cerebral ischemia in rats. Acta Pharmacol Sin 2003; 24: 796-804.

[14] Zhang T, Jia W and Sun X. 3-n-Butylphthalide (NBP) reduces apoptosis and enhances vascular endothelial growth factor (VEGF) up-regulation in diabetic rats. Neurol Res 2010; 32: 390-396.

[15] Li J, Li Y, Ogle M, Zhou X, Song M, Yu SP and Wei L. DL-3-n-butylphthalide prevents neuronal cell death after focal cerebral ischemia in mice via the JNK pathway. Brain Res 2010; 1359: 216-226.

[16] Zhao CY, Lei H, Zhang Y, Li L, Xu SF, Cai J, Li PP, Wang L, Wang XL and Peng Y. L-3-n-Butylphthalide attenuates neuroinflammatory responses by downregulating JNK activation and upregulating Heme oxygenase-1 in lipopolysaccharide-treated mice. J Asian Nat Prod Res 2016; 18: 289-302.

[17] Peng Y, Xing C, Lemere CA, Chen G, Wang L, Feng Y and Wang X. l-3-n-Butylphthalide ameliorates beta-amyloid-induced neuronal toxicity in cultured neuronal cells. Neurosci Lett 2008; 434: 224-229.

[18] Peng Y, Xing C, Xu S, Lemere CA, Chen G, Liu B, Wang L, Feng Y and Wang X. L-3-n-butylphthalide improves cognitive impairment induced by intracerebroventricular infusion of amyloid-beta peptide in rats. Eur J Pharmacol 2009; 621: 38-45.

[19] Feng X, Peng Y, Liu M and Cui L. DL-3-n-butylphthalide extends survival by attenuating glial activation in a mouse model of amyotrophic lateral sclerosis. Neuropharmacology 2012; 62: 1004-1010.

[20] Zhou KL, Zhou YF, Wu K, Tian NF, Wu YS, Wang YL, Chen DH, Zhou B, Wang XY, Xu HZ and Zhang XL. Stimulation of autophagy promotes functional recovery in diabetic rats with spinal cord injury. Sci Rep 2015; 5: 17130.

[21] Feng ZC, Donnelly L, Li J, Krishnamurthy M, Riopel M, Wang R. Critical role of c-Kit in beta cell function: increased insulin secretion and protection against diabetes in a mouse model. Diabetologia 2012; 55: 2214-2225.

[22] Feng ZC, Riopel M, Li J, Donnelly L, Wang R. Downregulation of Fas activity rescues early onset of diabetes in c-Kit(Wv/+) mice. Am J Physiol Endocrinol Metab 2013; 304: E557-565.

[23] Feng ZC, Donnelly L, Li J, Krishnamurthy M, Riopel M, Wang R. Inhibition of Gsk3beta activity improves beta-cell function in c-KitWv/+ male mice. Lab Invest 2012; 92: 543-555.

[24] Feng ZC, Popell A, Li J, Silverstein J, Oakie A, Yee SP, Wang R. c-Kit receptor signaling regulates islet vasculature, beta-cell survival, and function in vivo. Diabetes 2015; 64: 3852-3866.

[25] Li J, Feng ZC, Yeung FS, Wong MR, Oakie A, Fellows GF, Goodyer CG, Hess DA, Wang R. Aldehyde dehydrogenase 1 acitivity in the developing human pancreas modulates retinoic acid signaling in mediating islet differentiation and survival. Diabetologia 2014; 57: 754-764.

[26] Zhang HY, Zhang X, Wang ZG, Shi HX, Wu FZ, Lin BB, Xu XL, Wang XJ, Fu XB, Li ZY, Shen CJ, Li XK and Xiao J. Exogenous basic fibroblast growth factor inhibits ER stress-induced apoptosis and improves recovery from spinal cord injury. CNS Neurosci Ther 2013; 19: 20-29.

[27] Deng W and Feng Y. Effect of dl-3-n-butylphthalide on brain edema in rats subjected to focal cerebral ischemia. Chin Med Sci J 1997; 12: 102-106.

[28] Chong ZZ and Feng YP. dl-3-n-butylphthalide attenuates reperfusion-induced blood-brain barrier damage after focal cerebral ischemia in rats. Zhongguo Yao Li Xue Bao 1999; 20: 696-700.

[29] Liu XG and Feng YP. Protective effect of dl-3-n-butylphthalide on ischemic neurological damage and abnormal behavior in rats subjected to focal ischemia. Yao Xue Xue Bao 1995; 30: 896-903.

[30] Lin JF and Feng YP. Effect of dl-3-n-butylphthalide on delayed neuronal damage after focal cerebral ischemia and intrasynaptosomes calcium in rats. Yao Xue Xue Bao 1996; 31: 166-170.

[31] Huai Y, Dong Y, Xu J, Meng N, Song C, Li W and Lv P. L-3-n-butylphthalide protects against vascular dementia via activation of the Akt kinase pathway. Neural Regen Res 2013; 8: 1733-1742.

[32] Wang F, Ma J, Han F, Guo X, Meng L, Sun Y, Jin C, Duan H, Li H and Peng Y. DL-3-n-butylphthalide delays the onset and progression of diabetic cataract by inhibiting oxidative stress in rat diabetic model. Sci Rep 2016; 6: 19396.

[33] Dai Z, Xiao J, Liu SY, Cui L, Hu GY and Jiang DJ. Rutaecarpine inhibits hypoxia/reoxygenation-induced apoptosis in rat hippocampal neurons. Neuropharmacology 2008; 55: 1307-1312.

[34] Zhou Y, Zhang H, Zheng B, Ye L, Zhu S, Johnson NR, Wang Z, Wei X, Chen D, Cao G, Fu X, Li X, Xu HZ and Xiao J. Retinoic acid induced-autophagic flux inhibits ER-Stress dependent apoptosis and prevents disruption of blood-spinal cord barrier after spinal cord injury. Int J Biol Sci 2016; 12: 87-99.

[35] Kuang X, Hu W, Yan M and Wong PK. Phenylbutyric acid suppresses protein accumulation-mediated ER stress in retrovirus-infected astrocytes and delays onset of paralysis in infected mice. Neurochem Int 2010; 57: 738-748.

[36] Mecha M, Torrao AS, Mestre L, Carrillo-Salinas FJ, Mechoulam R and Guaza C. Cannabidiol protects oligodendrocyte progenitor cells from inflammation-induced apoptosis by attenuating endoplasmic reticulum stress. Cell Death Dis 2012; 3: e331.

[37] Zhang H, Wu F, Kong X, Yang J, Chen H, Deng L, Cheng Y, Ye L, Zhu S, Zhang X, Wang Z, Shi H, Fu X, Li X, Xu H, Lin L and Xiao J. Nerve growth factor improves functional recovery by inhibiting endoplasmic reticulum stress-induced neuronal apoptosis in rats with spinal cord injury. J Transl Med 2014; 12: 130.

[38] Hu J, Wen Q, Wu Y, Li B and Gao P. The effect of butylphthalide on the brain edema, blood-brain barrier of rats after focal cerebral infarction and the expression of Rho A. Cell Biochem Biophys 2014; 69: 363-368.